11th ANKARA INTERNATIONAL AEROSPACE CONFERENCE **AIAC-2021-080**
8-10 September 2021 - METU, Ankara TURKEY

# A CASE STUDY OF AIRFOIL AEROACOUSTICS CHARACTERISTICS IN-FLIGHT ICING CONDITIONS

Ömer Akbal[1] and Erdem Ayan[2]
Turkish Aerospace
Ankara, Turkey

Baha Zafer[3]
Istanbul Technical University
Istanbul, Turkey

## ABSTRACT

*The purpose of the study is to determine aeroacoustics response of NACA0012 with and without icing conditions numerically. In order to validate the followed methodology, experimental data is used. FENSAP ICE tool is utilized to calculate ice accretion. On the other hand, for acoustic analyses, Unsteady Reynolds Averaged Navier Stokes (URANS) is used to initialize the simulation. Obtaining unsteady field data, Large Eddy Simulation (LES) and Stress Blended Eddy Simulation (SBES) RANS-LES model are carried out using combined with flow domain results and Ffowcs Williams-Hawkings (FW-H) method. For the sound pressure level (SPL), LES model showed better agreement with the experimental result rather than SBES, whereas SBES model has capability to consider ice roughness effects. It is concluded that icing on airfoil leads to increase boundary layer thickness and brings about more interaction on turbulent wake region. The peak SPL value is calculated as 53.36 dB at 800 Hz in normal (without icing) condition whereas in icing condition with same configuration, it is calculated as 61.54 dB in 1 kHz at low temperature icing condition and 55.70 dB in 0.8 kHz around freezing temperature icing condition. For the acoustics analogy in icing condition at low temperature condition, 8-10 dB increase in SPL is seen between 10 kHz to 100k kHz, whereas around freezing temperature condition, its value is oscillated more and 8-10 dB increased in noticed in between 25 kHz to 100 kHz.*

## INTRODUCTION

In-flight icing can be a serious threat to flight safety and it has several significant effects. Aerodynamic performance degradation and decreasing stall angle make more compelling for the takeoff and landing phases in flight envelope. The accumulation of ice on the aircraft can also disrupt the flow field pattern, causing increase in drag and decrease in lift force [Cebeci and Besnard, 1994]. At present, there are several methods for the challenging of the aircraft icing phenomenon with using ice detection try to avoid icing conditions and/or activate ice protection systems. The fund of knowledge of aircraft icing and safety concerns, airfoil profile has frequently used in icing studies by researchers. Furthermore, icing has significant effects

[1] Turkish Aerospace, Email: omer.akbal@tai.com.tr
[2] Turkish Aerospace, Email: eayan@tai.com.tr
[3] Associate Professor in a Department, Email: zaferba@itu.edu.tr

on the surface roughness of the airfoil that also effect boundary layer interaction and aerodynamic performance.

Recently, researchers have investigated unsteady flow feature of icing profile through experimental and numerical due to the separation region and turbulent effect of icing. Gurbacki and Bragg examined transient flow feature of icing profile via visualization analysis [Gurbacki and Bragg, 2004]. According to researcher finding, flow field are exposed to more vortex zone due to ice shapes and bring about separation region and re-attachment of boundary layer.

In addition, airfoil has self-noise characteristics with the interaction between airfoil structure and their turbulence produced in the boundary layer and near wake region. Airfoil and its boundary layer interaction creates to airfoil self-noise [Brooks, 1989]. The self-noise mechanisms produced by the airfoil have been occurred in several conditions and they are adapted from Brooks study, which are the interaction between turbulent boundary layer and trailing edge wake region, laminar boundary layer with vortex region, boundary layer separation at trailing edge especially high angle of attack and tip vortex formation noise. Separation stall noise with large scale and boundary layer separation are illustrated in Figure-1.

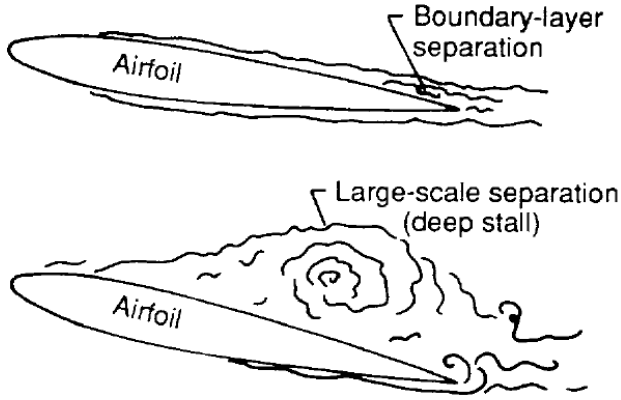


Figure 1: Separation-stall noise on airfoil [Brooks, 1989]

Besides, with the vortex interaction and more turbulent region in iced airfoil, icing is considered as the additional sources for airfoil self-noise, therefore, it is required to examine aerodynamic and aeroacoustics characteristics of an icing profile to determine icing effect in acoustic analyses.

In 2016, Szasz et al conducted acoustic simulation for iced airfoil at low mach number with combined LES and FW-H equation. It is seen that iced airfoil shows about the decreasing low frequency noise rather than clean airfoil [Szasz et al, 2016]. In 2016, Cheng et al performed experimental study about noise emitted from blade surface roughness of icing blade in rotorcraft. It was obtained that trailing edge noise was the main source. Additionally, if the surface roughness increases, rotor broadband noise also increases due to the interaction between increasing boundary layer and turbulence intensity [Cheng et al, 2016]. In 2020, Bao et al studied the effects of icing profile on aeroacoustics. Horn icing shape with its height, angle and location were found important differences in terms of aeroacoustics between icing airfoil and clean airfoil [Bao et al, 2020].

In this study, flow field study was performed for 3-D NACA 0012 and flow conditions in order to compute aerodynamically generated sound for clean and icing conditions. Numerical analysis of icing profile was obtained with using FENSAP ICE. LES and SBES are performed with FW-H equation for the acoustic analogy to determine numerical methods in acoustic analyses.

# METHOD

## Aerodynamic Analogy

Flow field prediction study is the first step analysis for icing and aeroacoustics analyses steps to determine required velocity and pressure distributions. For the validation study, Ladson study is used as experimental data for lift coefficient (Ladson, 1988). The accuracy of the flow field resolution affects the acoustic results since the acoustic model depends on the correct prediction of the boundary layer behavior and the resulting surface pressure distributions on the airfoil. Flow field validation is performed with $2x10^6$ Reynolds number. The generated mesh is structured and the first grid point near the wall has a $y^+$, which is between 0.5 and 1 around the airfoil. The aerodynamic validation in terms of $C_L$ - AoA is shown in Figure 2

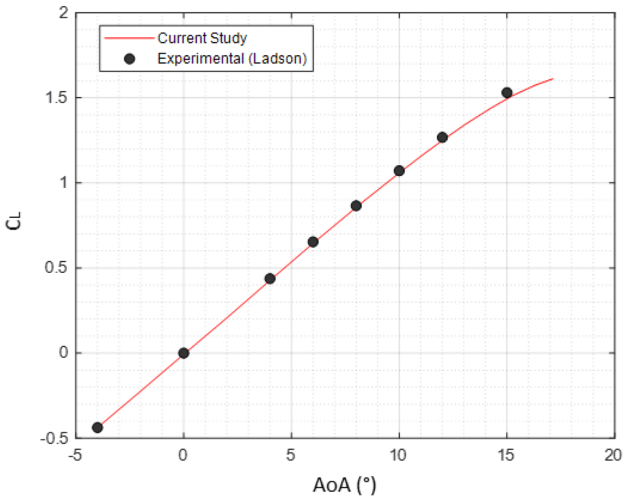


Figure 2: Lift coefficient – Angle of Attack validation for NACA0012

## Icing Analogy

Icing validation study is performed on NACA0012, which has 0.53 m chord. Experimental data is gathered from NASA technical report (Wright et al, 1997). Two operating icing conditions are selected and tabulated in Table 1. Airfoil geometry, angle of attack, air speed, air temperature, liquid water content, droplet diameter, humidity, pressure and exposure time are the fundamental parameters for icing calculation.

Table 1*:* Experimental operating conditions for icing validation case

| Angle of Attack (°) | Velocity (m/s) | Tstatic (°C) | Ttotal (°C) | Pressure (kPa) | LWC (g/m3) | Exposure Time (s) |
|---|---|---|---|---|---|---|
| 4 | 58.1 | -26.8 | -26 | 95.61 | 1,3 | 480 |
| 4 | 58.1 | -6.6 | -2 | 95.61 | 1,3 | 480 |

Flow field study is the first step of icing calculation to determine velocity and pressure distributions. Then, droplet trajectories calculations are performed to obtain collection efficiency parameter. Last step is to calculate ice thickness on airfoil by using energy equations. FENSAP ICE module is used for these calculations. Eulerian approach is selected for simulating the two-phase flow for icing simulations. In Figure 3, the results of the both conditions numerical results are compared in terms of the ice shapes at mid-span locations. In each case, multi-shot approach is used and it is observed that all the predictions agree fairly well.

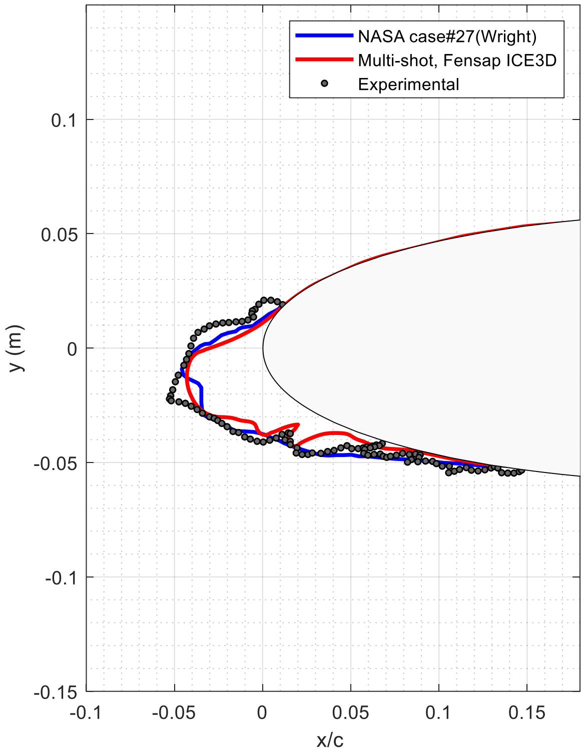


(a)

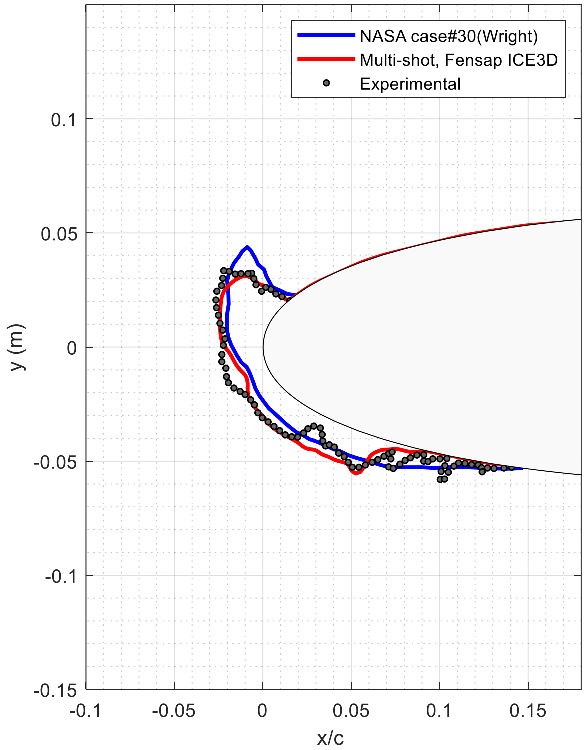


(b)

Figure 3: *Ice accretion* on NACA0012 both (a) Case#27 and (b) Case#30

For the droplet impingement analysis, DROP3D module is used to calculate collection efficiency around airfoil. Monodisperse method is selected for the droplet distribution as 20 $\mu$. ICE3D module is used to calculate ice accretion around airfoil. When the ice grows on airfoil, the mesh around airfoil changes due to contaminated ice and modifies transport of air and water droplets around airfoil. Therefore, multi-shot approach is used to compute more realistic and accurate ice shapes. The exposure time of icing is divided into smaller steady state intervals. A several studies are performed to obtain acceptable ice shapes which are compatible with experimental results. According to the calculated ice thicknesses on airfoil, ice accretion process is divided into 6 layers. Additionally, the airfoil surface roughness is calculated as 0.5 mm which is compatible with Shin et al study [Shin et al, 1991].

## Acoustic Analogy

Acoustic simulations are performed using FW-H equation to predict airfoil self-noise. The numerical algorithm is performed for the validation of acoustic analogy for NACA 0012 using experimental report. RANS analyses is performed to initialize the simulation for steady calculations. Then, LES and SBES models are used for the unsteady simulations to determine acceptable model by considering computational cost and accuracy.

Used simulation domain is shown in Figure 4. The experimental profile NACA0012 have 0.2286 m chord and 0.4586 m span, however in this study span is taken 10 % chord which contribute to 0.02286 m for capturing the span-wise flow field characteristics to reduce computational cost. Reynolds number is calculated as 6.2x10$^5$ based on freestream velocity 39.6 m/s that corresponds to Mach number as 0.115.

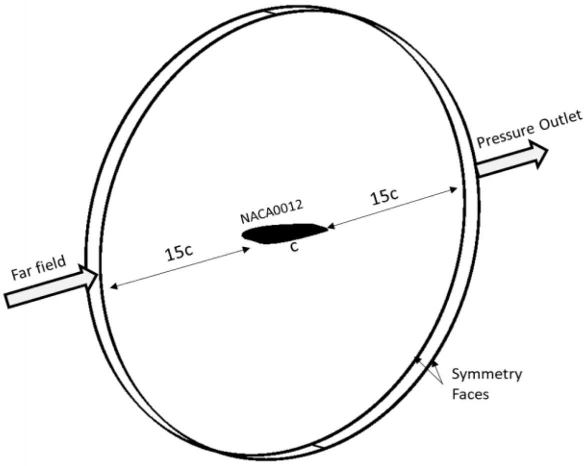


Figure 4: Circular domain used for the aeroacoustics simulations including the boundary conditions

The grids are created in an iterative process which are suitable for the acoustics application. O-grid analogy is used and the total distance of grid is equal to 30 chord length. Grid on the airfoil is achieved using hyperbolic function. The grid distribution over the airfoil is not symmetric, and more points are distributed over the suction section of the airfoil to have higher resolution. Trailing edge of the airfoil is rounded to be compatible with O-grid analogy as given in Figure 5-c. The inflation layer is refined to achieve $y^{+} \leq 1$ for the first layer on the wall. 450 nodes along the chord-wise and 150 nodes along the span-wise are used. The resulting complete mesh includes approximately 15 million grid as illustrated in Figure 5.

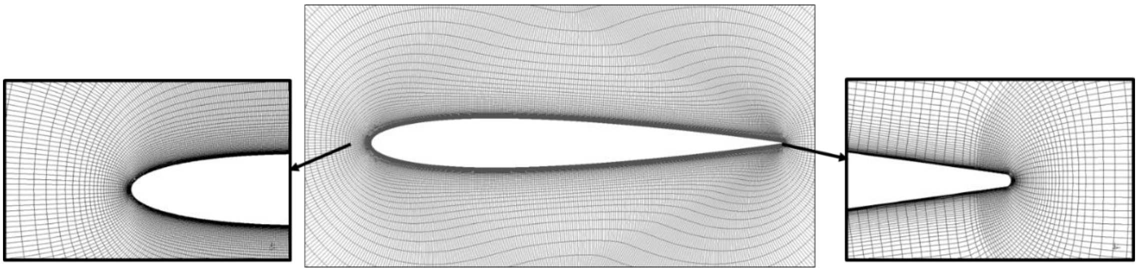

(a) (b) (c)

Figure 5: O type structured grid for NACA 0012 normal conditions (a) Leading edge (b) Overall (c) Rounded trailing edge

LES method could give better prediction of broadband noise under different incoming flow conditions (Chen, 2021). In the LES method, the Smagorinsky–Lilly subgrid-scale model is used to simulate the subgrid-scale eddy viscosity. The three-dimensional simulation is started from a spanwise extruded two-dimensional solution. The pressure outlet boundary condition with 1 atm is adopted on the outlet, the non-slip wall boundary condition is imposed on the airfoil, and the symmetry boundary conditions are adopted in the spanwise direction. All calculations are performed in parallel mode with 200 cores provided by Turkish Aerospace.

The PISO algorithm (Pressure Implicit with Splitting of Operator (Issa, 1986)) is used for the transient simulations with pressure and momentum second order equations. Pressure far field boundary condition is used. The green-gause node method is performed to utilize the pressure gradient. Time step size is determined as $5\times10^{-6}$ s to maintain CFL number smaller than 1 in all fluid domain. Non dimensional convective time is utilized as 2. An acoustic receiver is located at a point in the mid-span plane 1.2 m from the trailing edge of the airfoil perpendicular to the chord line to match the position of the microphone to recreate same setup experimental study [Brooks, 1989].

Figure 6 shows the shear stress behavior on the surface of the NACA0012. Shear stress has a strong demonstration of the boundary layer behavior. Turbulence region is occurred at the 20 % chord of the airfoil as shown in Figure 6.

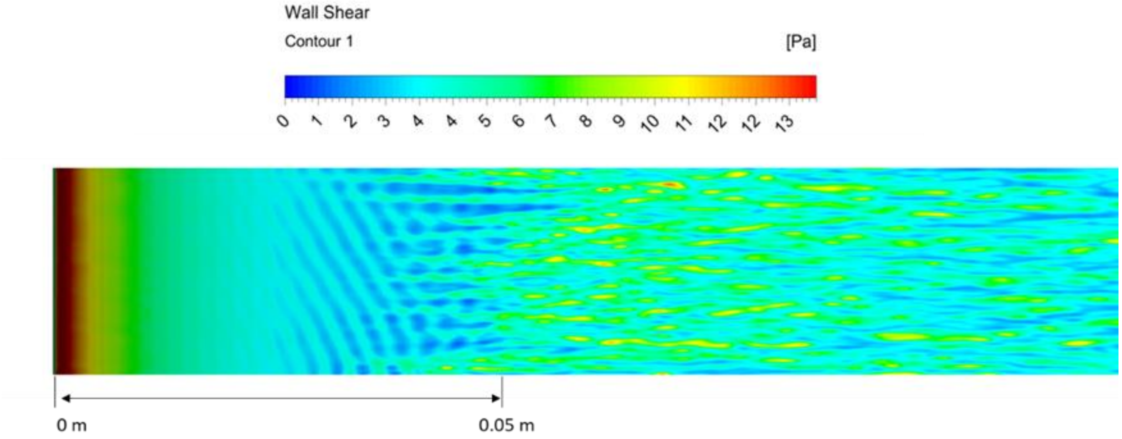


Figure 6: Wall shear stress contours from 0 to 15 Pa for NACA0012

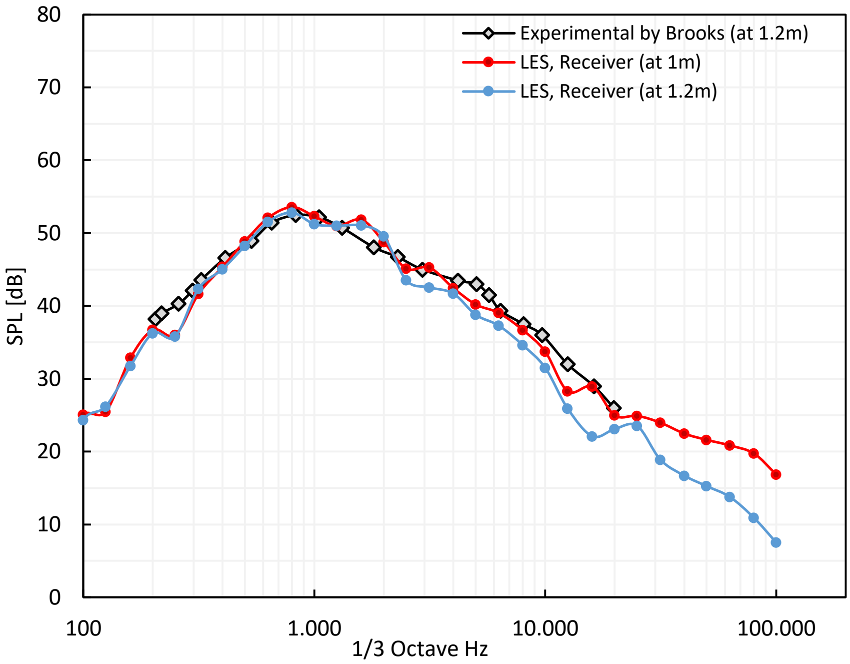


Figure 7: Acoustic analogy validation using LES at 0°angle of attack of one-third octave SPL ref. 20 μ Pa.

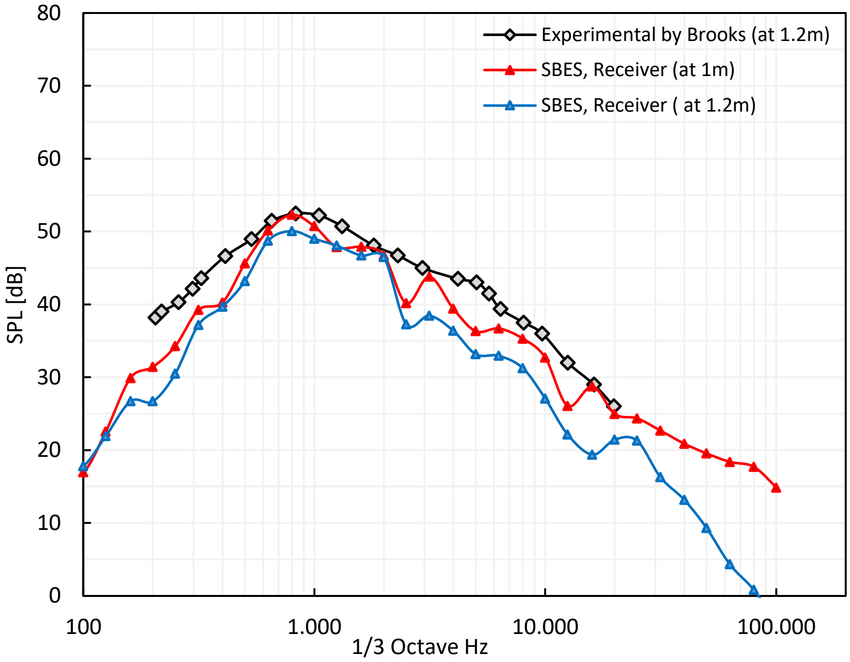


Figure 8: Acoustic analogy validation using SBES at 0°angle of attack of one-third octave SPL ref. 20 µ Pa.

Large eddy simulation is performed and results are depicted in Figure 7. SBES model is also used and corresponding results are given in Figure 8. It is concluded that LES simulation SPL value has similar trend and well compatible with experimental results along the all frequencies range rather than SBES model. The experimental acoustic result by Brooks corresponds from 20 Hz to 20 kHz frequencies range. Numerical result for LES simulation is well captured by these frequencies range. For the Overall SPL in dB (reference pressure = $2x10^{-5}$) are calculated as 60.05 dB and 58.36 dB for LES and SBES, respectively. Besides, peak values for both model and their results are tabulated in Table 2.

Table 2: SPL peak values for both numerical and experimental results.

| Model | Normal Conditions | |
|---|---|---|
| | Peak Frequency | SPL (dB) |
| LES | 800 Hz | 53.60 |
| SBES | 800 Hz | 50.10 |
| Experimental | 850 Hz | 52.48 |

### Acoustic in Icing Condition

Aeroacoustics study in icing condition are analyzed with same parameters as acoustic validation case. The reference chord is 0.2286 m and velocity is 39.6 m/s at zero angle of attack. Two icing conditions are modeled for acoustic calculation. Icing condition is adapted from Appendix-C intermittent maximum. Icing exposure time is selected as 300 seconds, 500-meter altitude, and has 20-µ droplet monodisperse diameter. The first condition corresponds to -20°C and the second one is to -3°C. Liquid water content is calculated from Appendix-C condition and LWC are 1.48 g/m$^3$ and 1.7 g/m$^3$ for -20°C and -3°C air temperature, respectively. All acoustic setup has same acoustic analogy with validation study. Calculated ice accreted shapes on airfoil are shown in Figure 9-a for two different conditions at 0° AoA. The iced profile has same grid configuration with non-iced condition. Leading edge grid distribution at low temperature case is illustrated in Figure 9-b.

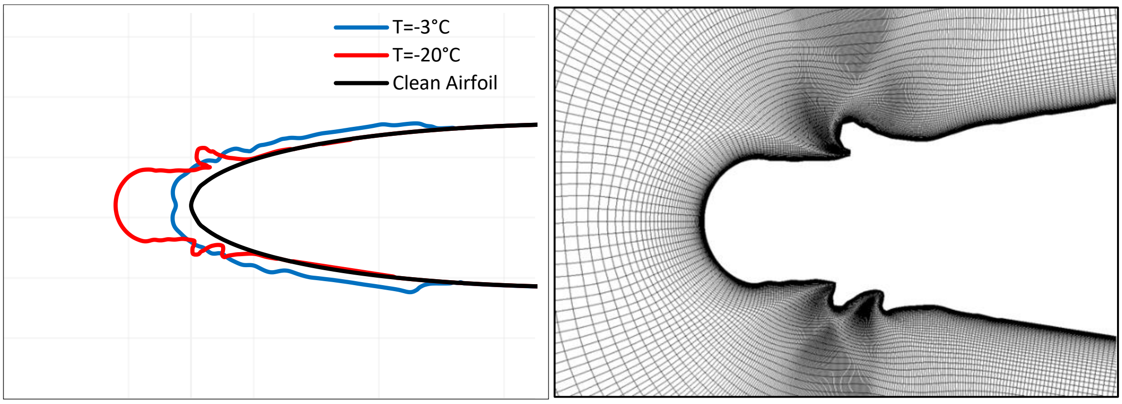


(a) (b)

Figure 9: (a) Ice accretion on NACA0012 in icing conditions (b) generated grid distribution on leading edge of iced profile for acoustic calculation

The type of the boundary layer (laminar or turbulent) is conditioned by the Reynolds number. In this study, Reynolds number is $6.2 \times 10^5$ for acoustic analysis. Turbulent boundary layer is providing to increase acoustic noise with interaction turbulent wake region. For this reason, boundary layer thickness for both conditions are calculated in three lines in this study. Line 1 corresponds to the line towards to the leading edge, Line 2 is generated at mid chord and Line 3 is near to the trailing edge as shown in Figure 10. Table 3 summarizes the boundary layer thickness at both normal and icing conditions for these three lines. Boundary layer thickness is increased to 47.5 % and 72.8 % for -3°C and -20°C icing conditions, respectively.

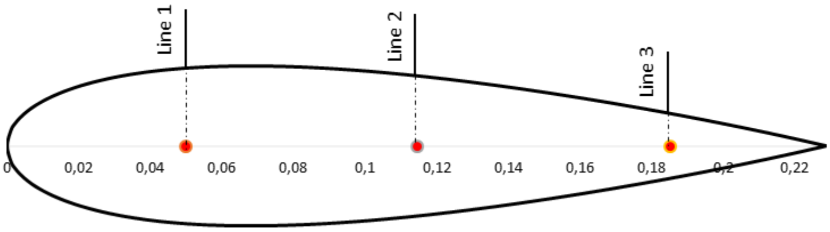


Figure 10: Schematic drawing of three lines for the boundary layer thickness calculation

Table 3: Boundary layer thickness values

| | Line 1 | Line 2 | Line 3 |
|---|---|---|---|
| | **Boundary Layer (m)** | **Boundary Layer (m)** | **Boundary Layer (m)** |
| Normal Conditions | 0,00077 | 0,00252 | 0,00423 |
| Icing Conditions T=-3°C | 0,00359 | 0,00480 | 0,00696 |
| Icing Conditions T=-20°C | 0,00677 | 0,00927 | 0,01134 |

Figure 11 shows boundary layer heights in icing conditions along the Line 2. It is obtained that ice accretion on airfoil brings about increasing boundary layer thickness, which result in also increased acoustic noise in this study.

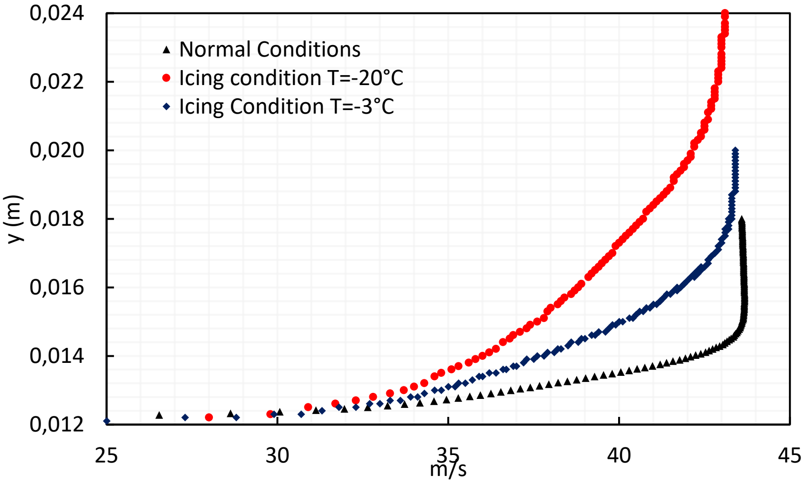


Figure 11: Boundary layer calculation lines on airfoil along the Line 2.

For iced profile, results show that ice mainly accumulates at leading edge of the airfoil, which effects the stagnation location and flow separation regions along pressure and suction sides. Thicker boundary layer profile is obtained in case of iced airfoil for both conditions (Figure 11). It results in important change in the aerodynamic characteristics of the airfoil. Velocity contours for both normal and iced airfoils are illustrated in Figure 12.

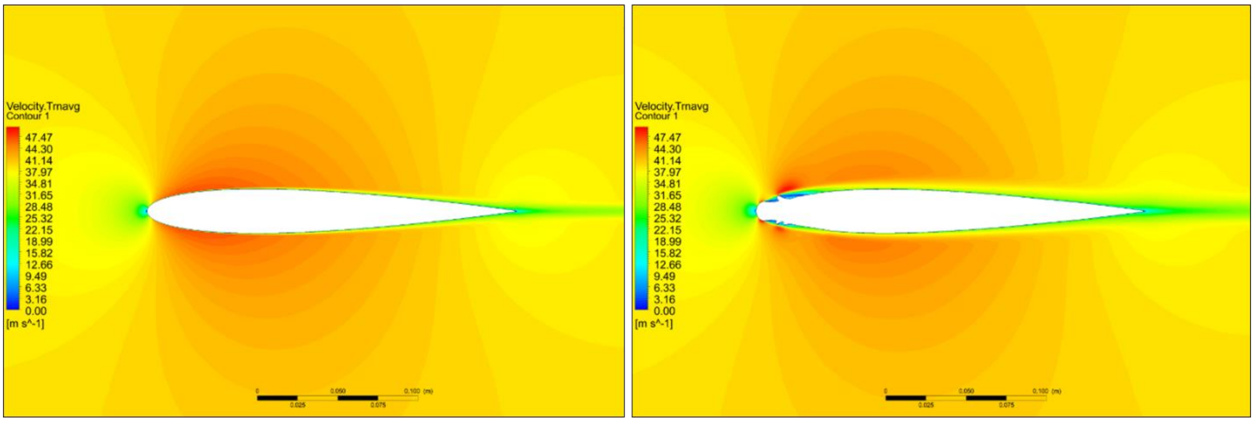


(a) (b)

Figure 12: Mean Velocity Contour for normal and icing condition (-20°C)

Figure 13 shows vorticity contours at the mid-span of iced NACA0012 airfoil. The bigger vortices are occurred in iced section at the region of the separation bubble. Upper and lower airfoil surfaces have similar vortex structures due to zero angle of attack condition.

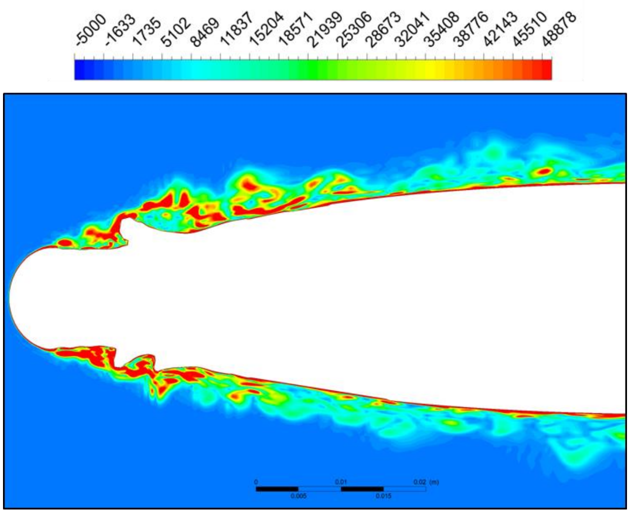


Figure 13: Spanwise vorticity contour of iced NACA0012

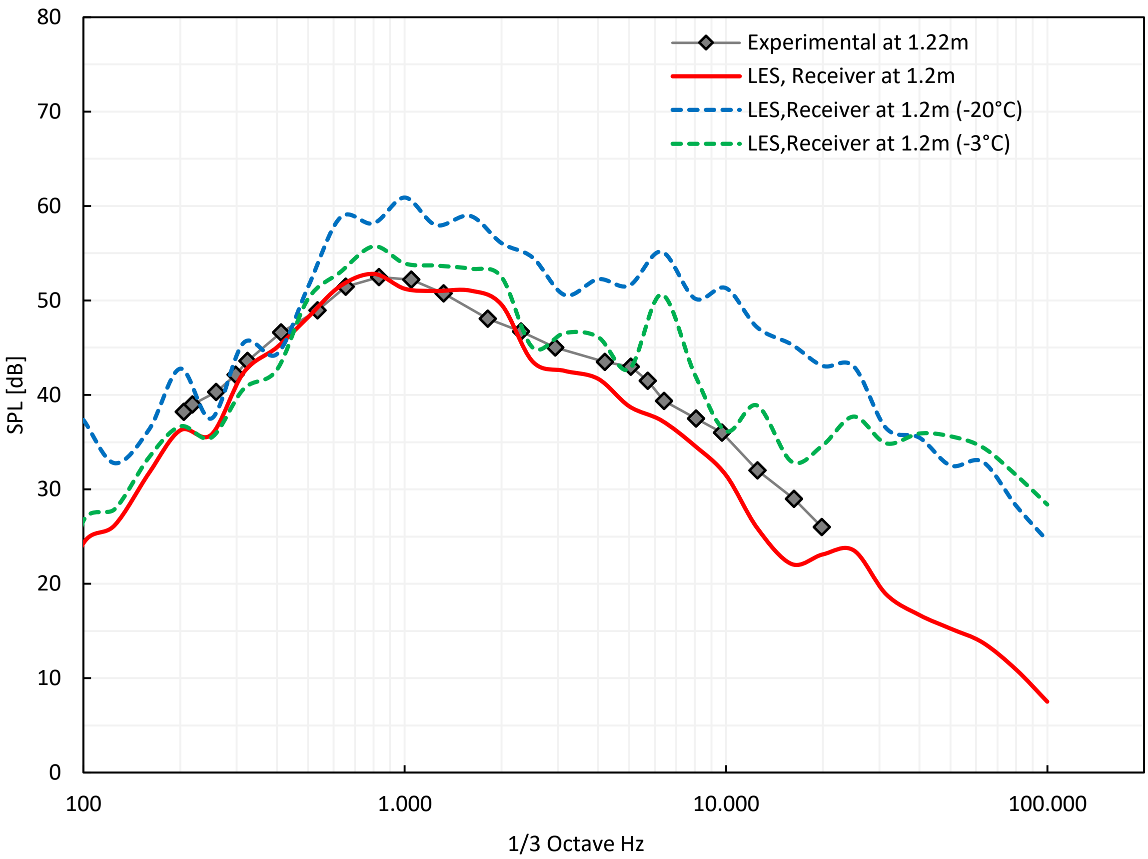


Figure 14: Acoustic analogy using LES at 0°angle of attack of one-third octave SPL ref. 20 μ Pa. for both icing condition.

Overall SPL for normal and icing conditions are 60.04 dB, 67.88 dB (-20°C) and 62.83 Db (-3°C) respectively. In Figure 14, it is concluded that icing has much more effect in SPL at high frequency range between 10 kHz to 100 kHz, which demonstrate that turbulent effect is more dominant in icing conditions rather than normal conditions due to the high frequency – turbulence relation. However, in low frequency range (0.1 to 1 kHz), there is no significance change for both normal and icing conditions.

## CONCLUSION

This study intent to analyze the aeroacoustics response of NACA0012 with and without icing conditions numerically. Commercial icing tool FENSAP-ICE is used for numerical analyses and the resulting ice shapes are compared with the experimental data in the literature. LES is performed for acoustic analogy and well compatible with experimental results along the SPL-Frequency range. Ice accretion on airfoil resulted in to increase in boundary layer thickness, which caused more interaction on turbulent wake region and noise generation. Analyses demonstrated an important change in aerodynamic characteristics of NACA0012 after ice accretion, which brings an increase in the noise generation. It is concluded that the sound pressure level is nearly 8-10 dB higher in the high frequency region (10 kHz - 100 kHz) in the icing conditions that contributes to more turbulent effect.
These results showed the possibility of using acoustic responses to detect icing conditions. Additionally, roughness of iced airfoil will be modeled in the CFD analyses as well to examine its effect on flow behavior to capture more realistic results in next studies.

**ACKNOWLEDGE**
The authors are thankful for the computational resources of High Performance Computing Center which provided by Turkish Aerospace.

## References

Bao, S., Shi, Y., and Song, W. (2020) Numerical Study of Iced Airfoil Aeroacoustics using IIDES, AIAA Aviation Forum, June 2020

Brooks, T.F, Pope, D.S, and Marcolini, M.A.. (1989) Airfoil Self-Noise and Prediction. NASA RP1218

Cheng, B., Han, Y., Brentner, K. S., Palacios, J., and Morris, P. J., (2016) Rotor broadband noise due to surface roughness during ice accretion. 54C_ AIAA Aerospace Sciences Meeting, 2016, p. 1270.

Chen, N., Liu, H. (2021), Effects and mechanisms of LES and DDES method on airfoil self-noise prediction at low to moderate Reynolds numbers.

Cebeci, T., and Besnard, E. (1994) Prediction of the Performance Degradation of Aircraft in Natural Icing Conditions, AIAA Paper 94-0487.

Ffowcs Williams, J. E., and Hawkings, D. L.. (1969) Sound generation by turbulence and surfaces in arbitrary motion. Philosophical Transactions of the Royal Society of London. Series A, Mathematical and Physical Sciences, Vol. 264, No. 1151, 1969, pp. 321–342.

Gurbacki, H., and Bragg, M. (2004) Unsteady flowfield about an iced airfoil. 42=3 AIAA aerospace sciences meeting and exhibit, 2004, p. 562.

Issa, R. I. (1986) Solution of the implicitly discretised fluid flow equations by operator-splitting. J. Comput. Phys. 62(1),40–65.

J. Shin, et al. (1991) Prediction of ice shapes and their effect on airfoil performance. NASA Technical Memorandum 103701

Ladson, C. L. (1988). Effects of Independent Variation of Mach and Reynolds Numbers on the Low Speed Aerodynamic Characteristics of the NACA 0012 Airfoil Section

Szasz, R.-Z., Ronnfors, M., and Revstedt, J. (2016) Influence of ice accretion on the noise generated by an airfoil section. International Journal of Heat and Fluid Flow, Vol. 62, 2016, pp. 83 92.

Wasala, S.H., Storey, R. C., Norris, S. E., and Cater, J.E. (2015). Aeroacustic noise prediction for wind turbines using Large Eddy Simulation. Journal of Wind Engineering and Industrial Aerodynamics.